HHS Public Access

Author manuscript

J Biomol NMR. Author manuscript; available in PMC 2015 November 01.

Published in final edited form as:

J Biomol NMR. 2014 November ; 60(0): 189–195. doi:10.1007/s10858-014-9858-7.

NMR Structure Note: Solution structure of the free Zα domain of human DLM-1 (ZBP1/DAI), a Z-DNA binding domain

Yunhuang Yang[1], **Theresa A. Ramelot**[1], **Hsiau-Wei Lee**[2], **Rong Xiao**[3], **John K. Everett**[3], **Gaetano T. Montelione**[3,4], **James H. Prestegard**[2], and **Michael A. Kennedy**[1,*]

[1]Department of Chemistry and Biochemistry, and the Northeast Structural Genomics Consortium, Miami University, Oxford, Ohio, USA, 45056, United States

[2]Complex Carbohydrate Research Center, and the Northeast Structural Genomics Consortium, University of Georgia, Athens, Georgia, USA, 30602, United States

[3]Department of Molecular Biology and Biochemistry, and the Northeast Structural Genomics Consortium, Center for Advanced Biotechnology and Medicine, Rutgers, The State University of New Jersey, Piscataway, New Jersey 08854, United States

[4]Department of Biochemistry, Robert Wood Johnson Medical School, University of Medicine and Dentistry of New Jersey, Piscataway, New Jersey 08854, United States

Keywords

Solution structure; free Zα domain; DLM-1; Z-DNA binding domain

Biological context

The protein DLM-1 (also called Z-DNA binding protein 1, ZBP1) is the product of the *dlm-1* gene. The *dlm-1* gene was initially isolated and identified using the RNA differential display technique where they found that it was highly up-regulated in the peritoneal lining tissue of mice bearing nearby ovarian tumors and in activated macrophages (Fu et al. 1999). DLM-1 was proposed to play a role in host defense against tumors, although its precise function was unknown (Fu et al. 1999). In 2001, the N-terminal domain of mouse DLM-1 ($Z\alpha_{DLM-1}$) was co-crystallized with left-handed Z-DNA (PDB ID 1J75) (Schwartz et al. 2001). The complex structure revealed that $Z\alpha_{DLM-1}$ is structurally similar to the Zα domain of double-stranded RNA adenosine deaminase ADAR1 ($Z\alpha_{ADAR1}$), the first crystal structure of a protein bound to left-handed Z-DNA (PDB ID 1QBJ) (Schwartz et al. 1999), although they only share about 35% amino acid sequence identity (Schade et al. 1999; Schwartz et al. 1999). Human ADAR1 and its chicken homologue have also exhibited high Z-DNA binding affinity (Herbert et al. 1997; Herbert et al. 1995). In 2007, DLM-1 was found to be an innate immune activator, capable of sensing cytosolic DNAs exposed in a cell by infection or by incomplete clearance during cell damage (Takaoka et al. 2007). In response to foreign DNA, DLM-1 can activate type I interferon (IFN) and other genes

*Correspondence to: Michael A. Kennedy, Department of Chemistry and Biochemistry, Miami University, Oxford, Ohio 45056, Phone: +1 523 529 8267, Fax: +1 513 529 5715, kennedm4@miamioh.edu.

involved in innate immunity. Therefore, this protein was alternatively named DAI (*D*NA-dependent *a*ctivator of *I*NF-regulatory factors) in light of its newly revealed cellular biological function. For consistency, this protein (DLM-1/ZBP1/DAI) will be referred to as DLM-1 in this structure note report.

Full length DLM-1 contains four domains (Rothenburg et al. 2002): two tandem homologs of Z-DNA binding domains, $Z\alpha_{DLM-1}$ and $Z\beta_{DLM-1}$, followed by a B-DNA binding domain, and a C-terminal domain. The mechanism of DLM-1 activation has been well studied after it was identified as the first innate immune activator that senses cytosolic DNA. By binding to double-stranded DNA with its N-terminal domains, DLM-1 enhances its intermolecular associations with the IRF 3 (IFN regulatory factor) transcription factor and TBK 1 (Tank binding kinase) serine/threonine kinase with its C-terminus (~100 amino acids) (Takaoka et al. 2007). Further studies showed that all three DNA-binding domains are required for full activation of DLM-1 *in vivo*, and the dimerization of DLM-1 has been suggested to result in activation of the immune response at the molecular level (Wang et al. 2008). At the cellular level, the localization of DLM-1 and its association with stress granules is regulated by Z-DNA binding domains (Deigendesch et al. 2006; Pham et al. 2006).

To date, mouse $Z\alpha_{DLM-1}$ (Schwartz et al. 2001) and human $Z\beta_{DLM-1}$ (Ha et al. 2008; Ha et al. 2006; Kim et al. 2011) have been characterized in structural studies. The complex crystal structure of mouse $Z\alpha_{DLM-1}$ bound to Z-DNA revealed that $Z\alpha_{DLM-1}$ adopted a winged helix-turn-helix fold with an α/β architecture consisting of three α-helices and three β-strands, very similar to Z-DNA binding protein human $Z\alpha_{ADAR1}$. Both structures exhibited a common conserved domain core, and a protein-Z-DNA interface, which specifically bind Z-DNA by way of conserved positively charged and polar residues that play critical roles in recognition of the zig-zag conformation of the Z-DNA phosphodiester backbone (Schade et al. 1999); (Schwartz et al. 2001; Schwartz et al. 1999). NMR spectroscopy revealed that $Z\alpha_{ADAR1}$ is also capable of binding B-DNA and then converting it to Z-DNA, which suggested an active B-Z DNA transition mechanism (Kang et al. 2009). Further studies on $Z\alpha_{ADAR1}$ indicated that it binds Z-DNA using a distinct conformation in a highly flexible region of the protein, the β1-loop-α2 segment, and that $Z\alpha_{ADAR1}$ undergoes conformational change as it binds B-DNA with lower affinity compared to with Z-DNA (Lee et al. 2012). As a homolog of $Z\alpha_{DLM-1,}$ human $Z\beta_{DLM-1}$ has a similar structural fold, but shows significant variation in the sequence of the residues that are essential for Z-DNA binding (Ha et al. 2008). In addition, chemical shift perturbation experiments using NMR spectroscopy revealed that $Z\beta_{DLM-1}$ binds weakly to B-DNA (Kim et al. 2011). The solution structure of the N-terminal domain of the vaccinia virus E3L also exhibited a structural similarity to human $Z\alpha_{ADAR}$ and mouse $Z\alpha_{DLM-1}$ and exhibited Z-DNA binding affinity (Kahmann et al. 2004).

The human cancer pathway protein interaction network (HCPIN) was constructed by the Northeast Structural Genomics Consortium (NESG) (Huang et al. 2008) to identify proteins relevant to cancer biology as targets for three-dimensional structural determination. DLM-1, initially identified as a gene product up-regulated in murine stromal cells lining tumors, was one of the HCPIN proteins targeted for structure determination by NESG. Although the structure of mouse $Z\alpha_{DLM-1}$ bound to Z-DNA has been characterized, the three-dimensional

structure of free human $Z\alpha_{DLM-1}$ has not been previously reported. The proteins share only 66% sequence identity. In this study, we cloned the DNA encoding human $Z\alpha_{DLM-1}$ (6–74) on chromosome 20 orf183, and solved its solution structure by NMR. The structure exhibited similarity to its mouse counterpart in complex with Z-DNA, and has a corresponding binding surface for Z-DNA.

Methods and results

Protein expression, purification and NMR samples preparation

The DNA encoding human $Z\alpha_{DLM-1}$ (6–74) was cloned into an NESG-modified pET15 expression vector derivative with a short N-terminal hexaHis affinity purification tag (MGHHHHHHSH) (Acton et al. 2005). Following NESG standard protocols (Acton et al. 2011), $Z\alpha_{DLM-1}$ was expressed and purified to prepare U-^{13}C, ^{15}N (NC) and U-^{15}N, 5% biosynthetically-directed ^{13}C (NC5) samples. NMR samples were purified using an ÄKTAxpress (GE Healthcare) with a Ni-affinity column (HisTrap HP IMAC column, 5 ml) followed by gel filtration chromatography (HiLoad 26/60 Superdex 75). The protein was concentrated to 1.0 mM in the NMR buffer containing 10% v/v D_2O: 20 mM 2-(N-morpholino)ethanesulfonic acid (MES), 100 mM NaCl, 5 mM $CaCl_2$, 10 mM DTT, 50 μM DSS, and 0.02% NaN_3 at pH 6.5. A D_2O-exchanged sample was prepared for HD exchange experiments by freezing the NC sample followed by lyophilization and resuspension in 99.9% D_2O (Acros Organics).

NMR spectroscopy data collection and assignments

NMR experiments were carried out at 298 K on a Varian Inova 600 MHz spectrometer with a 5-mm HCN cryogenic probe and Bruker Avance III 850 MHz spectrometer equipped with a conventional room temperature 5-mm HCN probe. ^{1}H, ^{13}C and ^{15}N chemical shifts were assigned from conventional triple-resonance spectra on NC sample including 2D ^{1}H-^{15}N HSQC and ^{1}H-^{13}C HSQC (aliphatic and aromatic), 3D HNCO, HNCA, HN(CO)CA, HNCACB, CBCA(CO)NH, HBHA(CO)NH, HC(C)H-COSY, HC(C)H-TOCSY and (H)CCH-TOCSY. Stereospecific isopropyl methyl assignments for all Val and Leu amino acids were deduced from characteristic cross-peak fine structures in a high-resolution 2D ^{1}H-^{13}C HSQC spectrum of NC5 sample (Neri et al. 1989). To obtain the NOE-based distance restraints required for the structure calculation, four NOESY spectra including 3D ^{15}N-edited NOESY-HSQC and ^{13}C-edited NOESY-HSQC (optimized for aliphatic or aromatic carbons) on the NC sample, and an additional 4D ^{13}C-^{13}C-HMQC-NOESY-HMQC on D_2O exchanged sample (99.9% D_2O) were collected with a 70 ms mixing time. These NOESY spectra were also analyzed to confirm side chain ^{1}H assignments. All NMR data were processed using NMRPipe and analyzed with the Sparky program. 2D ^{1}H-^{15}N HSQC spectrum of human $Z\alpha_{DLM-1}$ was well dispersed and almost completely assigned (Fig. 1). Final ^{1}H, ^{13}C and ^{15}N chemical shifts were deposited in the BioMagResBank (BMRB ID 18158).

Residual dipolar coupling

Backbone ^{1}H-^{15}N residual dipolar couplings (RDCs) for human $Z\alpha_{DLM-1}$ were measured on isotropic and aligned NC5 samples in 2D *J*-modulated spectra on a Varian Inova 600 MHz

spectrometer at 298 K (Tjandra et al. 1996). The protein was partially aligned in two alignment media $C_{12}E_5$ polyethylene glycol (PEG) and a positively charged polyacrylamide gel (Hansen et al. 1998; Ruckert and Otting 2000). In total, 95 RDC restraints (49 from PEG and 46 from gel) were used for the structure calculation and refinement calculations.

NMR structure calculation and refinement

NOE-based inter-proton distance restraints were determined automatically for $Z\alpha_{DLM-1}$ using CYANA 3.0 (Guntert 2004). Input for CYANA consisted of chemical shift assignments, NOESY peak lists from four NOESY spectra with peak intensities, the restraints for backbone phi (φ) and psi (ψ) torsion angle derived from chemical shifts of backbone atoms using the TALOS+ software program (Shen et al. 2009), and RDC restraints determined in PEG and gel aligned samples. Manual and iterative refinements of NOESY peak picking lists were guided using NMR RPF quality to assess “goodness of fit” between calculated structures and NOESY peak lists (Huang et al. 2005). Towards the end of the iterative structure calculation process, 22 x 2 hydrogen bond restraints for the NH-O and N-O distances were introduced based on identification of proximity of potential donors and receptors in early structure calculations and after confirmation from slow amide proton exchange based on HD exchange measurements. The 20 lowest energy structures calculated by CYANA 3.0 were further refined using restrained molecular dynamics in explicit water CNS 1.2 (Linge et al. 2003) and the PARAM19 force field, using the final NOE-derived distance constraints, TALOS-derived dihedral angle restraints and RDC restraints. The final NMR ensemble of 20 structures has been deposited in the Protein Data Bank (PDB ID 2LNB). The final restraints for structure calculation and refinement including NOE_based distance restraints, hydrogen bond restraints, dihedral angle restraints and RDC restraints have also been deposited in PDB and BMRB. Structural statistics and global structure quality factors were computed using PSVS version 1.4 (Table 1) (Bhattacharya et al. 2007).

Solution structure of human $Z\alpha_{DLM-1}$

Human $Z\alpha_{DLM-1}$ has a molecular weight of 9.0 kDa (including the 10-residue N-terminal tag). Analytical static light scattering measurements in-line with gel-filtration chromatography indicated that it was a monomer under the conditions used in the NMR experiments. In addition, the estimated overall isotropic rotational correlation time (τ_c) of 5.6 ± 0.5 ns, determined at 298 K based on ^{15}N relaxation times measured from 1D ^{15}N-edited T_1 and T_2 experiments (Kay et al. 1989), was consistent with a 9 kDa protein, confirmed its monomeric state. The chemical shift dispersion of the amide resonances in both ^{1}H and ^{15}N dimensions was characteristic of a folded protein in solution (Fig. 1).

The extensive and accurate assignment of the backbone and side chain ^{1}H, ^{13}C and ^{15}N chemical shifts (almost completely assigned except for the N-terminal tag residues) were crucial as initial experimental input for the automatic assignment of NOESY peaks during the iterative structure calculations using CYANA. The agreement between the final assigned 1562 NOESY peak list and the calculated structures was verified by the RPF software package (Huang et al. 2005) as indicated in Table 1. Figure 2a shows the superposition of the ordered regions of the final ensemble of 20 calculated structures, which have a RMSD of 0.4 Å for backbone atoms and 1.0 Å for all heavy atoms.

Figure 2b shows a ribbon representation of the lowest energy structure of human $Z\alpha_{DLM-1}$ from the ensemble. All secondary elements in the ensemble were well defined including three helices colored yellow (α1: R10-A25, α2: L31-C38, and α3: K42–K54) and three strands colored blue (β1: V29-K30, β2: V58-S62, and β3: T65-L68), which were sequentially arranged with the order: α1-β1-α2-α3-β2-β3. The overall structure of human $Z\alpha_{DLM-1}$ is winged helix-turn-helix fold. The hydrophobic core was formed with three helices packed against three antiparallel β-strands. Helices 2 and 3 formed the helix-turn-helix unit with helix 1 joined to helix 2 by a short β-strand, β1. The 'wing' consisted of the C-terminal of helix 3 and the β-sheet formed by three antiparallel β-strands in the order of β1-β3-β2.

Discussion and conclusions

Full-length mouse DLM-1 (UniprotKB ID Q9QY24) contains 411 amino acids with a molecular weight of 44.3 kDa (Fu et al. 1999), whereas the human counterpart (UniprotKB ID Q9H171) has 429 amino acids with molecular weight of 46.3 kDa. While the full-length human protein has a sequence identity of 50% to its mouse homolog, its N-terminal domain, $Z\alpha_{DLM-1}$, shares a higher sequence identity of 66%. The human $Z\alpha_{DLM-1}$ exhibits high structural similarity to its mouse counterpart with a small RMSD of 0.79 Å for backbone atoms in the ordered region (Fig. 2C). The structural alignment reveals that free $Z\alpha_{DLM-1}$ exhibits a surface poised for binding to Z-DNA, as well as critically positioned charged and polar residues on helix-3, a characteristic that is also found in the other Z-DNA proteins and which mediates electrostatic and polar interactions that promote binding to the zig-zag phosphodiester backbone of the Z-DNA. Similar observations have been made regarding the human RNA editing enzyme ADAR1 as well (Schade et al. 1999). The structural similarities support that human $Z\alpha_{DLM-1}$ plays a similar role in Z-DNA binding as its mouse counterpart.

Sequence conservation of the $Z\alpha_{DLM-1}$ family was analyzed using ConSurf (Ashkenazy et al. 2010; Glaser et al. 2003). Sequence alignment of five $Z\alpha_{DLM-1}$ homologs is shown in Figure 3a with secondary structural elements for human $Z\alpha_{DLM-1}$ depicted above the sequence alignment and conserved residues colored red. As indicated in Figure 3b, all 12 conserved residues appear in the ordered region. These conserved residues likely play an important role in maintaining the protein fold and for recognition of Z-DNA. Electrostatic surface potentials computed using APBS (Baker et al. 2001) show that six positively charged residues are present in the region of Z-DNA binding (Fig. 3C) based on overlay with the structure of the mouse $Z\alpha_{DLM-1}$ bound to Z-DNA. The crystal structural of mouse $Z\alpha_{DLM-1}$ bound to Z-DNA showed that three residues N46, Y50 and W50 made up the core protein-DNA binding interface, and conserved positively charged residues such as K42 and K43 played a role in contacting the RNA sugar-phosphate backbone (Schwartz et al. 2001). By sequence and structure alignments, all these residues are identical in both the mouse and human homologs except for R43 in human $Z\alpha_{DLM-1}$ that is conserved as K43 in the mouse and other mammalian homologs.

In summary, the proposed biochemical function of human $Z\alpha_{DLM-1}$ involved in Z-DNA binding is supported by its structural similarity to other authenticated Z-DNA binding

proteins. Furthermore, based its the structural similarity to mouse $Z\alpha_{DLM-1}$, the human $Z\alpha_{DLM-1}$ exhibits a surface that is not only complementary to the structure of Z-DNA and which is poised to bind to Z-DNA, but that also exhibits several charged and polar residues correctly positioned to make electrostatic and interactions with the zigzag conformation of phosphodiester backbone of Z-DNA in the region of α3 and β-hairpin (β2 and β3). These same charged and polar residues likely drive the B-DNA to Z-DNA transition observed for Z-DNA binding proteins (Kang et al., 2009) by promoting initial weak binding to B-DNA through non-optimal electrostatic and polar interactions due to the differences in the B-DNA shape in comparison to the optimal Z-DNA structure, which is followed by the conformational transition to the relatively high energy Z-DNA structure that is associated with very tight binding.

Acknowledgments

This work was supported by the National Institute of General Medical Sciences; Protein Structure Initiative-Biology Program; Grant Number: U54-GM074958 and U54-GM094597. We thank K. Hamilton, E. Kohan, D. Wang, and T. Acton at the Rutgers' protein production facility for technical support. All NMR data collection was conducted at the Ohio Biomedicine Center of Excellence for Structural Biology and Metabonomics at Miami University.

References

Acton TB, Gunsalus KC, Xiao R, Ma LC, Aramini J, Baran MC, Chiang YW, Climent T, Cooper B, Denissova NG, Douglas SM, Everett JK, Ho CK, Macapagal D, Rajan PK, Shastry R, Shih LY, Swapna GV, Wilson M, Wu M, Gerstein M, Inouye M, Hunt JF, Montelione GT. Robotic cloning and Protein Production Platform of the Northeast Structural Genomics Consortium. Methods Enzymol. 2005; 394:210–243. [PubMed: 15808222]

Acton TB, Xiao R, Anderson S, Aramini J, Buchwald WA, Ciccosanti C, Conover K, Everett J, Hamilton K, Huang YJ, Janjua H, Kornhaber G, Lau J, Lee DY, Liu G, Maglaqui M, Ma L, Mao L, Patel D, Rossi P, Sahdev S, Shastry R, Swapna GV, Tang Y, Tong S, Wang D, Wang H, Zhao L, Montelione GT. Preparation of protein samples for NMR structure, function, and small-molecule screening studies. Methods Enzymol. 2011; 493:21–60. [PubMed: 21371586]

Ashkenazy H, Erez E, Martz E, Pupko T, Ben-Tal N. ConSurf 2010: calculating evolutionary conservation in sequence and structure of proteins and nucleic acids. Nucleic Acids Res. 2010; 38:W529–533. [PubMed: 20478830]

Baker NA, Sept D, Joseph S, Holst MJ, McCammon JA. Electrostatics of nanosystems: application to microtubules and the ribosome. Proc Natl Acad Sci U S A. 2001; 98:10037–10041. [PubMed: 11517324]

Bhattacharya A, Tejero R, Montelione GT. Evaluating protein structures determined by structural genomics consortia. Proteins. 2007; 66:778–795. [PubMed: 17186527]

Deigendesch N, Koch-Nolte F, Rothenburg S. ZBP1 subcellular localization and association with stress granules is controlled by its Z-DNA binding domains. Nucleic Acids Res. 2006; 34:5007–5020. [PubMed: 16990255]

Fu Y, Comella N, Tognazzi K, Brown LF, Dvorak HF, Kocher O. Cloning of DLM-1, a novel gene that is up-regulated in activated macrophages, using RNA differential display. Gene. 1999; 240:157–163. [PubMed: 10564822]

Glaser F, Pupko T, Paz I, Bell RE, Bechor-Shental D, Martz E, Ben-Tal N. ConSurf: identification of functional regions in proteins by surface-mapping of phylogenetic information. Bioinformatics. 2003; 19:163–164. [PubMed: 12499312]

Guntert P. Automated NMR structure calculation with CYANA. Methods Mol Biol. 2004; 278:353–378. [PubMed: 15318003]

Ha SC, Kim D, Hwang HY, Rich A, Kim YG, Kim KK. The crystal structure of the second Z-DNA binding domain of human DAI (ZBP1) in complex with Z-DNA reveals an unusual binding mode to Z-DNA. Proc Natl Acad Sci U S A. 2008; 105:20671–20676. [PubMed: 19095800]

Ha SC, Van Quyen D, Hwang HY, Oh DB, Brown BA 2nd, Lee SM, Park HJ, Ahn JH, Kim KK, Kim YG. Biochemical characterization and preliminary X-ray crystallographic study of the domains of human ZBP1 bound to left-handed Z-DNA. Biochim Biophys Acta. 2006; 1764:320–323. [PubMed: 16448869]

Hansen MR, Mueller L, Pardi A. Tunable alignment of macromolecules by filamentous phage yields dipolar coupling interactions. Nat Struct Biol. 1998; 5:1065–1074. [PubMed: 9846877]

Herbert A, Alfken J, Kim YG, Mian IS, Nishikura K, Rich A. A Z-DNA binding domain present in the human editing enzyme, double-stranded RNA adenosine deaminase. Proc Natl Acad Sci U S A. 1997; 94:8421–8426. [PubMed: 9237992]

Herbert A, Lowenhaupt K, Spitzner J, Rich A. Chicken double-stranded RNA adenosine deaminase has apparent specificity for Z-DNA. Proc Natl Acad Sci U S A. 1995; 92:7550–7554. [PubMed: 7638229]

Huang YJ, Hang D, Lu LJ, Tong L, Gerstein MB, Montelione GT. Targeting the human cancer pathway protein interaction network by structural genomics. Mol Cell Proteomics. 2008; 7:2048–2060. [PubMed: 18487680]

Huang YJ, Powers R, Montelione GT. Protein NMR recall, precision, and F-measure scores (RPF scores): structure quality assessment measures based on information retrieval statistics. J Am Chem Soc. 2005; 127:1665–1674. [PubMed: 15701001]

Kahmann JD, Wecking DA, Putter V, Lowenhaupt K, Kim YG, Schmieder P, Oschkinat H, Rich A, Schade M. The solution structure of the N-terminal domain of E3L shows a tyrosine conformation that may explain its reduced affinity to Z-DNA in vitro. Proc Natl Acad Sci U S A. 2004; 101:2712–2717. [PubMed: 14981270]

Kang YM, Bang J, Lee EH, Ahn HC, Seo YJ, Kim KK, Kim YG, Choi BS, Lee JH. NMR spectroscopic elucidation of the B-Z transition of a DNA double helix induced by the Z alpha domain of human ADAR1. J Am Chem Soc. 2009; 131:11485–11491. [PubMed: 19637911]

Kay LE, Torchia DA, Bax A. Backbone dynamics of proteins as studied by 15N inverse detected heteronuclear NMR spectroscopy: application to staphylococcal nuclease. Biochemistry. 1989; 28:8972–8979. [PubMed: 2690953]

Kim K, Khayrutdinov BI, Lee CK, Cheong HK, Kang SW, Park H, Lee S, Kim YG, Jee J, Rich A, Kim KK, Jeon YH. Solution structure of the Z beta domain of human DNA-dependent activator of IFN-regulatory factors and its binding modes to B- and Z-DNAs. Proceedings of the National Academy of Sciences of the United States of America. 2011; 108:6921–6926. [PubMed: 21471454]

Lee AR1, Kim HE, Lee YM, Jeong M, Choi KH, Park JW, Choi YG, Ahn HC, Choi BS, Lee JH. NMR dynamics study of the Z-DNA binding domain of human ADAR1 bound to various DNA duplexes. Biochem Biophys Res Commun. 2012; 428:137–41. [PubMed: 23079620]

Linge JP, Williams MA, Spronk CA, Bonvin AM, Nilges M. Refinement of protein structures in explicit solvent. Proteins. 2003; 50:496–506. [PubMed: 12557191]

Neri D, Szyperski T, Otting G, Senn H, Wuthrich K. Stereospecific nuclear magnetic resonance assignments of the methyl groups of valine and leucine in the DNA-binding domain of the 434 repressor by biosynthetically directed fractional 13C labeling. Biochemistry. 1989; 28:7510–7516. [PubMed: 2692701]

Pham HT, Park MY, Kim KK, Kim YG, Ahn JH. Intracellular localization of human ZBP1: Differential regulation by the Z-DNA binding domain, Zalpha, in splice variants. Biochem Biophys Res Commun. 2006; 348:145–152. [PubMed: 16876127]

Rothenburg S, Schwartz T, Koch-Nolte F, Haag F. Complex regulation of the human gene for the Z-DNA binding protein DLM-1. Nucleic Acids Res. 2002; 30:993–1000. [PubMed: 11842111]

Ruckert M, Otting G. Alignment of biological macromolecules in novel nonionic liquid crystalline media for NMR experiments. J Am Chem Soc. 2000; 122:7793–7797.

Schade M, Turner CJ, Kuhne R, Schmieder P, Lowenhaupt K, Herbert A, Rich A, Oschkinat H. The solution structure of the Zalpha domain of the human RNA editing enzyme ADAR1 reveals a

prepositioned binding surface for Z-DNA. Proc Natl Acad Sci U S A. 1999; 96:12465–12470. [PubMed: 10535945]

Schwartz T, Behlke J, Lowenhaupt K, Heinemann U, Rich A. Structure of the DLM-1-Z-DNA complex reveals a conserved family of Z-DNA-binding proteins. Nat Struct Biol. 2001; 8:761–765. [PubMed: 11524677]

Schwartz T, Rould MA, Lowenhaupt K, Herbert A, Rich A. Crystal structure of the Zalpha domain of the human editing enzyme ADAR1 bound to left-handed Z-DNA. Science. 1999; 284:1841–1845. [PubMed: 10364558]

Shen Y, Delaglio F, Cornilescu G, Bax A. TALOS plus : a hybrid method for predicting protein backbone torsion angles from NMR chemical shifts. J Biomol Nmr. 2009; 44:213–223. [PubMed: 19548092]

Takaoka A, Wang Z, Choi MK, Yanai H, Negishi H, Ban T, Lu Y, Miyagishi M, Kodama T, Honda K, Ohba Y, Taniguchi T. DAI (DLM-1/ZBP1) is a cytosolic DNA sensor and an activator of innate immune response. Nature. 2007; 448:501–505. [PubMed: 17618271]

Tjandra N, Grzesiek S, Bax A. Magnetic field dependence of nitrogen-proton J splittings in N-15-enriched human ubiquitin resulting from relaxation interference and residual dipolar coupling. J Am Chem Soc. 1996; 118:6264–6272.

Wang Z, Choi MK, Ban T, Yanai H, Negishi H, Lu Y, Tamura T, Takaoka A, Nishikura K, Taniguchi T. Regulation of innate immune responses by DAI (DLM-1/ZBP1) and other DNA-sensing molecules. Proc Natl Acad Sci U S A. 2008; 105:5477–5482. [PubMed: 18375758]

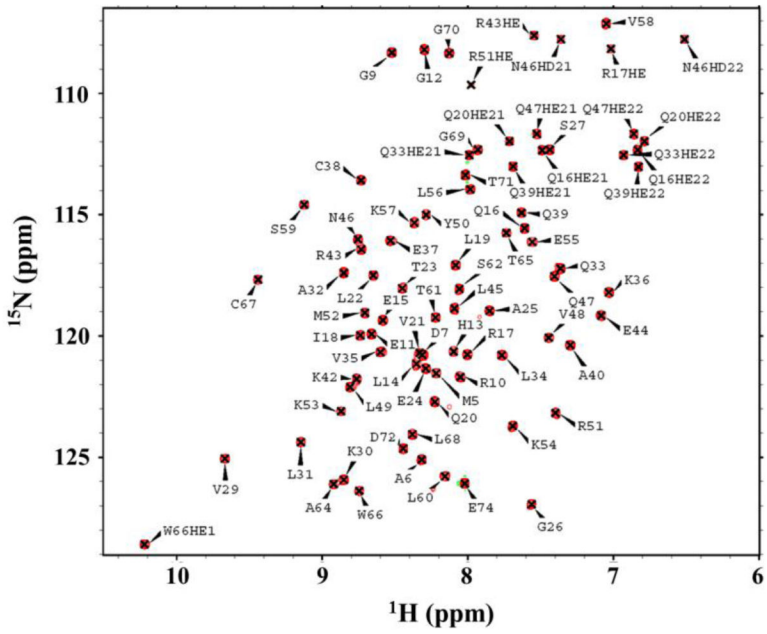

Fig. 1.

Assigned ^{1}H-^{15}N HSQC spectrum of ^{13}C, ^{15}N-labeled human $Z\alpha_{DLM-1}$ (1.0 mM) in NMR buffer collected at 298 K. Assigned side chain resonances of Arg (Hε/Nε, aliased), Trp (Hε1/Nε1), and side chain resonances of Asn and Gln (Asn Hδ2/Nδ2, and Gln Hε2/Nε2) are indicated.

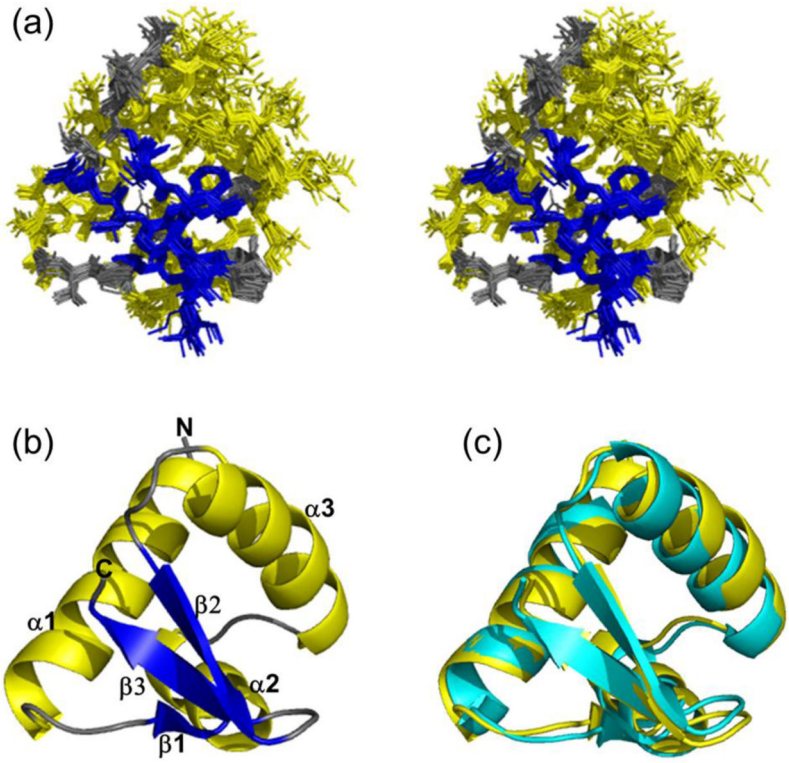

Fig. 2.

a Stereoview of the superimpositions of the 20 lowest energy structures of human $Z\alpha_{DLM-1}$. The three α-helices are colored yellow, three β-strands colored blue, and the N-terminal tail, C-terminal tail and loop regions are colored grey. The N-terminal hexaHis tags (MGHHHHHHSH) and the last five residues in C-terminus are not shown for clarity. **b** Ribbon diagram of the lowest energy structure of human $Z\alpha_{DLM-1}$. All secondary structural elements and N- and C-termini are labeled. **c** Overlay of ribbon structures of human $Z\alpha_{DLM-1}$ (yellow, lowest energy structure) and mouse $Z\alpha_{DLM-1}$ (cyan, PDB ID 1J75). Backbone RMSD in the ordered region (table 1) is about 0.79 Å (structure representative with the lowest energy for human $Z\alpha_{DLM-1}$).

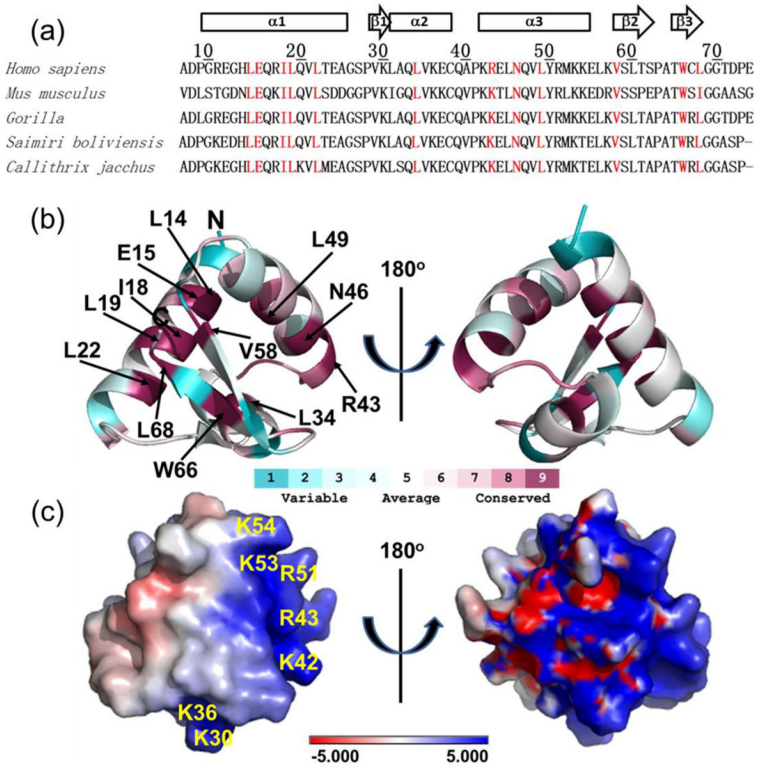

Fig. 3.

a Multiple amino acid sequence alignments of $Z\alpha_{DLM-1}$ in various mammalian organisms performed using clustalw2 (http://www.ebi.ac.uk/Tools/msa/clustalw2/). The sequence numbers and secondary structural elements of human $Z\alpha_{DLM-1}$ are indicated. α-helices are represented by tubes and β-strands by arrows. Highly conserved residues with score of 9 are color red. ConSurf analysis was performed using the first structure of human $Z\alpha_{DLM-1}$ as a query for homologs search with an E-value cut-off of 0.0001, maximal and minimal sequence identity of 95% and 35%, PSI-BLAST iteration number of three using a non-redundant sequence data bank. 49 unique sequences out of 80 PSI-BLAST hits were used for the conservation score calculation. **b** Amino acid conservation mapped onto the lowest energy NMR structure by Consurf analysis. **c** Solvent exposed electrostatic potential mapped onto the surface of human $Z\alpha_{DLM-1}$, computed for the first model of human $Z\alpha_{DLM-1}$ ensemble with the lowest energy using the APBS software package. Positively charged residues are indicated. The structure orientation is identical to that in **b**.

Table 1

Structure statistics for human Zα$_{\mathbf{DLM\text{-}1}}$[a]

Conformationally-restricting constraints [b]	
Distance constraints	
Intra-residue (i=j)	283
Sequential (|i-j|=1)	368
Medium-range (1<|i–j|<5)	397
Long-range (|i–j|≥5)	514
Total	1562
Hydrogen bond constraints	
Long-range (|i–j|≥5)/total	10/44
Dihedral angle constraints	94
NH RDC constraints (PEG/gel)	49/46
Residue constraint violations [b]	
Average number of distance violations per structure	
0.1–0.2Å	2.45
0.2–0.5 Å	0.3
>0.5Å	0
Average RMS distance violation/constraint (Å)	0.01
Maximum distance violation (Å)	0.24
Average number of dihedral angle violations per structure	
1–10°	1.55
>10°	0
Average RMS dihedral angle violation/constraint (degree)	0.3
Maximum dihedral angle violation (degree)	3.4
RDC Q_{rmsd} (PEG/gel)	0.17/0.16
RMSD from average coordinates [b,c]	
Backbone /Heavy atoms (Å)	0.4/1.0
Ramachandran plot statistics [b,c]	
Most favored regions (%)	99.6
Allowed regions (%)	0.4
Disallowed regions (%)	0
Global quality scores(raw/Z-score) [b]	
Verify3D	0.38/−1.28
Prosall	0.96/1.28
Procheck(phi-psi) [c]	0.28/1.42
Procheck(all) [c]	0.25/1.48
Molprobity clash	14.29/−0.93
RPF Scores [d]	
Recall	0.98
Precision	0.94

F-measure	0.96
DP-score	0.88

[a] Structure statistics were computed for the ensemble of 20 deposited structures.

[b] Calculated using PSVS 1.4 program. Residues (6–74) were analyzed.

[c] Ordered residues ranges (with sum of phi and psi > 1.8): 10–62, 65–68.

[d] RPF scores reflected the goodness-of-fit of the final ensemble of structures including disordered residues to the NMR data.